Stem Cell Reports
Report
OPEN ACCESS

Amelioration of Hyperbilirubinemia in Gunn Rats after Transplantation of Human Induced Pluripotent Stem Cell-Derived Hepatocytes

Yong Chen,[1,2] Yanfeng Li,[1,2] Xia Wang,[1,2] Wei Zhang,[2,3] Vanessa Sauer,[1,2] Chan-Jung Chang,[1] Bing Han,[5] Tatyana Tchaikovskaya,[1,2] Yesim Avsar,[1,2] Edgar Tafaleng,[5] Sanal Madhusudana Girija,[2,3] Krisztina Tar,[1,2] Zsuzsanna Polgar,[1,2] Stephen Strom,[6] Eric E. Bouhassira,[1] Chandan Guha,[2,3] Ira J. Fox,[5] Jayanta Roy-Chowdhury,[1,2,4,*] and Namita Roy-Chowdhury[1,2,4,*]

[1]Department of Medicine
[2]Marion Bessin Liver Research Center
[3]Departments of Radiation Oncology and Pathology
[4]Department of Genetics
Albert Einstein College of Medicine, Bronx, NY 10461, USA
[5]Department of Surgery and McGowan Institute for Regenerative Medicine, Children's Hospital of Pittsburgh, University of Pittsburgh Medical Center, Pittsburgh, PA 15224, USA
[6]Department of Laboratory Medicine, Karolinska Institute, 17177 Stockholm, Sweden
*Correspondence: jayanta.roy-chowdhury@einstein.yu.edu (J.R.-C.), namita.roychowdhury@einstein.yu.edu (N.R.-C.)
http://dx.doi.org/10.1016/j.stemcr.2015.04.017

SUMMARY

Hepatocyte transplantation has the potential to cure inherited liver diseases, but its application is impeded by a scarcity of donor livers. Therefore, we explored whether transplantation of hepatocyte-like cells (iHeps) differentiated from human induced pluripotent stem cells (iPSCs) could ameliorate inherited liver diseases. iPSCs reprogrammed from human skin fibroblasts were differentiated to iHeps, which were transplanted into livers of uridinediphosphoglucuronate glucuronosyltransferase-1 (UGT1A1)-deficient Gunn rats, a model of Crigler-Najjar syndrome 1 (CN1), where elevated unconjugated bilirubin causes brain injury and death. To promote iHep proliferation, 30% of the recipient liver was X-irradiated before transplantation, and hepatocyte growth factor was expressed. After transplantation, UGT1A1$^+$ iHep clusters constituted 2.5%–7.5% of the preconditioned liver lobe. A decline of serum bilirubin by 30%–60% and biliary excretion of bilirubin glucuronides indicated that transplanted iHeps expressed UGT1A1 activity, a postnatal function of hepatocytes. Therefore, iHeps warrant further exploration as a renewable source of hepatocytes for treating inherited liver diseases.

INTRODUCTION

Stem cells offer enormous promise as a source of differentiated cells for curing human diseases. Although liver transplantation is curative for life-threatening metabolic liver disorders (Åberg et al., 2011), minimally invasive catheter infusion of isolated hepatocytes into the liver can partially correct metabolic liver diseases and can greatly reduce the risk of fatal complications (Fox et al., 1998; Lysy et al., 2008; Roy-Chowdhury et al., 2009; Fisher and Strom, 2006). Host conditioning regimens developed in our laboratories (Guha et al., 2002) allow the expansion of engrafted donor hepatocytes, leading to complete cures of animal models of metabolic liver diseases. This host conditioning strategy is now being tested in a clinical hepatocyte transplant trial (University of Pittsburgh, Institutional Review Board [IRB] number PRO09040497).

Clinical application of hepatocyte transplantation has been impeded by the scarcity of donor livers, which are prioritized for organ transplantation. Pioneering studies have shown that somatic cells can be reprogrammed into induced pluripotent stem cells (iPSCs) that resemble embryonic stem cells (ESCs) (Takahashi and Yamanaka, 2006; Yu et al., 2007). Recent successes in differentiating ESCs and iPSCs into hepatocyte-like cells (iHeps) (Basma et al., 2009; Lavon et al., 2004; Schwartz et al., 2005; Cai et al., 2007; Duan et al., 2010; Si-Tayeb et al., 2010; Song et al., 2009) has opened the possibility of using iPSCs as a renewable source of human and, possibly, autologous hepatocytes.

Although iPSCs at various stages of differentiation have been reported to engraft and improve the survival of mice with severe toxic injury of the liver, neither the cause of death from the toxic liver injury nor the correction of any specific liver function by the engrafted cells has been demonstrated (Liu et al., 2011). In this study, we examined the efficacy of transplanting human iHep cells into Gunn rats, a well characterized animal model of Crigler-Najjar syndrome 1 (CN1) (Roy-Chowdhury et al., 1991, 1993). CN1 is an autosomal recessive disorder in which genetic lesions of *UGT1A1* cause life-long unconjugated hyperbilirubinemia because of a lack of uridinediphosphoglucuronate glucuronosyltransferase 1A1-mediated bilirubin glucuronidation by hepatocytes (Bosma et al., 1992). CN1 is lethal unless treated with life-long daily phototherapy to reduce bilirubin levels. Even with aggressive therapy, patients remain at risk of bilirubin encephalopathy and death. Liver transplantation is the only definitive therapy (Ozçay et al.,

2009). Gunn rats are well characterized animal models of CN1, with genetic and metabolic abnormalities similar to CN1 patients.

In this study, we transplanted human iHeps into the livers of Gunn rats. Proliferation of the transplanted cells was induced by preconditioning a single liver lobe by hepatic X-irradiation (HIR). HIR enhances the engraftment of transplanted cells by transiently disrupting the sinusoidal endothelial barrier. Additionally, reduction of the mitotic capacity of the irradiated host hepatocytes provides a competitive proliferative advantage to the engrafted cells (Guha et al., 2002; Yamanouchi et al., 2009). Here, as with patients, to increase the safety of HIR, we treated only one liver lobe, representing 30% of the liver mass, to achieve regional hepatic repopulation by the transplanted cells.

RESULTS AND DISCUSSION

Characteristics of Adult Human Skin Fibroblast-Derived iPSCs

iPSCs had a typical ESC-like morphology; expressed pluripotency markers (Figure S1A) at levels similar to those of the H1 hESC line (WiCell); differentiated spontaneously to cells of mesodermal, endodermal, and ectodermal origin (Figure S1B); and gave rise to teratomas after injection in severe combined immunodeficiency (SCID) mice (Figure S1C). iPSCs were diploid and contained 46 intact chromosomes (Figure S1D), and RT-PCR showed that exogenous *OCT-4*, *SOX2*, *KLF4*, and *c-MYC* were silenced (data not shown).

Directed Differentiation of Human iPSCs and Characteristics of iHeps

Undifferentiated iPSCs (Figure 1) expressed OCT-4 but there was very little expression of hepatocyte-preferred genes. After exposure to activin A and bFGF, OCT4 expression declined markedly, and the definitive endoderm marker SOX17 and the nuclear factor FOXA2 were expressed in 70%–85% of cells. The fetal hepatocyte marker α-fetoprotein (AFP) was expressed in 30%–50% of cells. After culturing with HGF and DMSO, AFP expression increased and human serum albumin (HSA) and CK18 were expressed. Following exposure to dexamethasone, the morphology of a majority of the cells changed toward that of primary human hepatocytes (Figures 2A–2C). A majority of these cells, termed iHeps, expressed HSA and cytokeratin 18, and less than half of the cells also expressed the asialoglycoprotein receptor (ASGPR), a marker of mature hepatocytes. AFP expression declined but was still seen in 1%–5% of cells (Figure 1). mRNA content measured by qRT-PCR showed gene expression of transcription factors that are important in hepatocyte development (e.g., HEX and PROX1) and maturation (e.g., HNF4α and C/EBPα) and secreted proteins as well as cytosolic, ER, plasma membrane, and peroxisomal proteins (Figure S2A). Confocal microscopy showed that ASGPR was distributed in both the plasma membranes and the cytoplasm (Figures S2B–S2D), whereas HSA was present in the cytoplasm (Figures S2E–S2G). In this cell population, some albumin-negative cells stained positive for SOX17, an early endodermal marker. SOX17 staining was absent or very faint in albumin-expressing cells (Figures S2H–S2K). Flow cytometry showed that 60%–90% of cells expressed HSA, whereas 28%–40% of cells expressed ASGPR (Figure 2D). At all stages, differentiation of iPSCs toward iHeps was similar to that seen with human embryonic stem cells (hESCs) (Basma et al., 2009). The iHeps exhibited hepatocyte-like characteristics, including glycogen storage (by periodic acid Schiff staining) (Figures 2E and 2F) and indocyanin green uptake (Figure 2I). They also showed uptake of dioctadecylindocarbocyanine (DiI)-labeled low-density lipoproteins (Figures 2G and 2H). Western blot analysis of cell homogenates confirmed that AFP appeared after iPSC exposure to activin A plus bFGF and increased after exposure to HGF and DMSO (Figure 2J). After exposure to dexamethasone, AFP decreased markedly. AFP was undetectable in mature primary hepatocytes. A trace of HSA was found in iPSCs and at the definitive endoderm stage (Figure 2J). HSA expression increased markedly after exposure to HGF plus DMSO. After exposure to dexamethasone, the HSA content reached 25% of that in freshly isolated primary human hepatocytes (Figure 2L).

In contrast to AFP and HSA, significant levels of UGT1A1 appeared only after exposure to HGF plus DMSO. Developmentally, UGT1A1 is expressed only with hepatocyte maturation after birth. After exposure to dexamethasone, the UGT1A1 content in iHeps increased markedly (Figure 2J), and UGT1A1 activity toward bilirubin was 18.8 ± 3.4 to 25.00 ± 4.6 pmole/min/mg protein (mean ± SD, n = 4), which is 18%–22% of the mean UGT1A1 activity in isolated normal primary human hepatocytes (Figure 2K).

As assessed by ELISA, the iHeps secreted the liver-specific proteins HSA, transferrin, and α-1-antitrypsin (AAT) into the culture medium at 33%, 46%, and 60% of the rate of secretion by primary human hepatocytes under identical conditions (Figures 2L–2N). iHeps secreted urea at approximately half the rate of primary human hepatocytes (Figure 2O). Undifferentiated iPSCs did not secrete HSA, AAT, transferrin, or urea (Figures 2K–2O).

Transplantation and Repopulation of Gunn Rat Livers with iHeps

Gunn rats were transplanted with 2×10^6 viable HSA-positive iHeps by intrasplenic injection as described

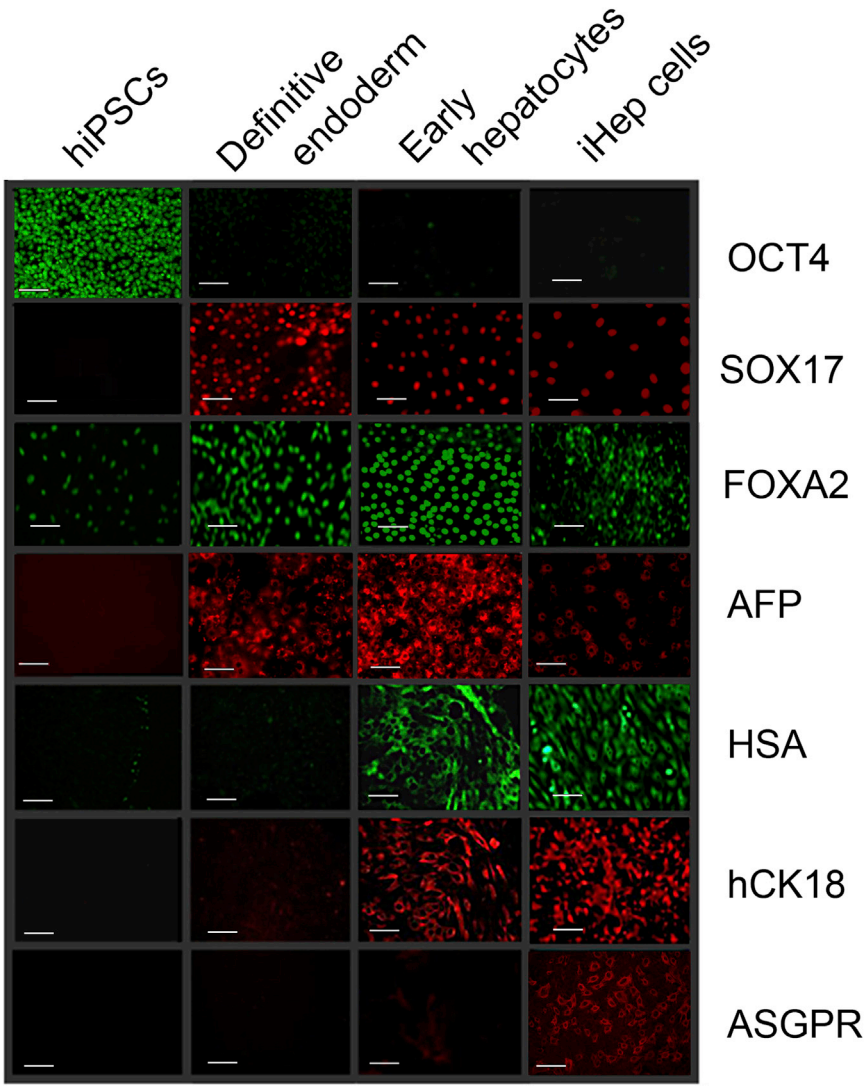

Figure 1. Expression of Cellular Marker Proteins during Differentiation of Human iPSCs

iPSCs were differentiated sequentially to definitive endoderm, early hepatocytes, and iHep cells as described in the text. Immunofluorescence staining for human OCT4, SOX17, FOXA2, AFP, HSA, CK18, and ASGPR is shown. Scale bars, 100 μm. See also Figure S1.

previously (Zhou et al., 2012). Because the rats are immune-competent, they were injected with tacrolimus (2 mg/kg subcutaneously daily) starting 7 days before transplantation to prevent xenograft rejection (Basma et al., 2009). For comparison, two rats received 2×10^6 human hepatocytes isolated from the livers of fumaryl acetoacetate hydrolase-deficient, Rag2$^{-/-}$, IL2-γc$^{-/-}$ (FRG) mice repopulated with human hepatocytes (purchased from Yecuris). To induce the preferential proliferation of transplanted cells, recipient rats received preparative HIR (50 Gy) to the median liver lobe, constituting 30% of the liver mass, on the day before transplantation and were injected with an adenoviral vector expressing HGF (10^{12} particles) 24 hr after the transplant (Zhou et al., 2012). Control rats (n = 4) received immunosuppression and HIR but were injected with saline instead of iHeps or primary hepatocytes.

Immunohistochemistry of liver sections of the preconditioned median lobe using a human UGT1A group-specific antibody showed clusters of human hepatocytes (Figures 3A and 3B) or iHep cells (Figures 3C–3E). A similar level of repopulation with iHeps was found by staining for HSA (Figures 2F and 2G). Image analysis using the ImageJ program showed that, 4-6 months after transplantation, the transplanted hepatocytes and iHeps comprised 17% ± 3.1% and 5.1% ± 2.6% (mean ± SD) of the hepatocyte mass, respectively (Figure 3H). In non-irradiated liver lobes, engrafted iHeps or primary human hepatocytes were seen as single cells or in groups of two to three cells (data not shown). Because hepatocytes engraft initially as single cells, the formation of human cell clusters indicated the proliferation of the engrafted cells in the preconditioned lobe. As expected, no human UGT1A-positive cells were found in control Gunn rat livers (data not shown). Liver

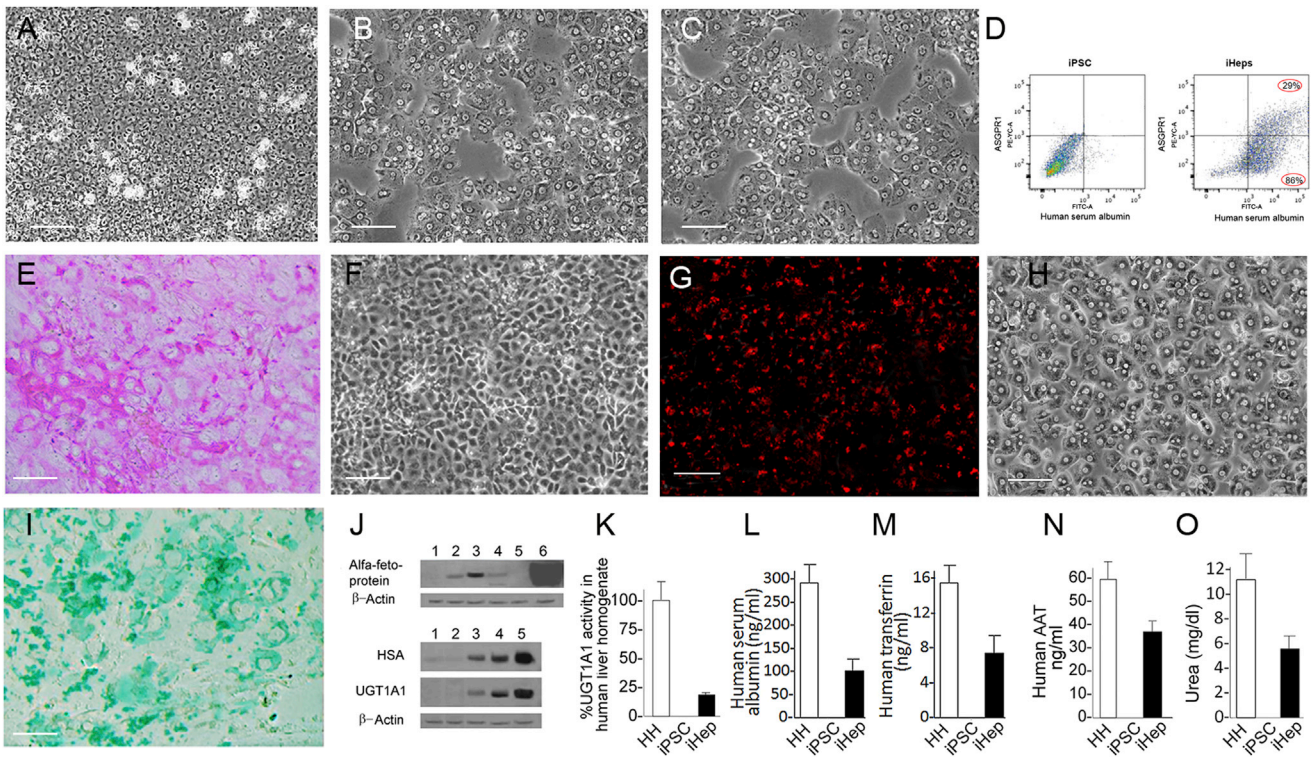

Figure 2. Characterization of the iHep Cells

The cells were differentiated in culture as described in Experimental Procedures.

(A–C) Phase contrast image of iPS cells, iHeps, and human primary hepatocytes, respectively. Scale bars, 100 μm.

(D) Flow cytometric analysis of HSA and ASGPR in iPSCs and iHeps. Scale bars, 100 μm.

(E) Periodic acid Schiff staining for glycogen content. Scale bars, 100 μm.

(F) Phase contrast image of (E).

(G) Uptake of DiI-LDL.

(H) Phase contrast image of (G).

(I) ICG uptake.

(J) Western blot for α-fetoprotein, human serum albumin, and UGT1A1: 1, undifferentiated human iPS; 2, definitive endoderm; 3, early hepatocytes; 4, hepatocyte-like cells (after exposure to dexamethasone); 5, human liver primary hepatocytes; 6, human hepatoma cell line HepG2.

(K) UGT1A1 activity toward bilirubin. The values are shown as percentage of the mean enzyme activity in homogenates of normal human liver specimens. Means of four determinations ± SD are shown. HH, primary human hepatocytes. The values are shown per million cells (means ± SD of data from four different iHep preparations).

(L–N) Secretion of human proteins into the media. After a fresh change of the serum-free culture medium, the cells were cultured for 24 hr, the media were harvested, and specific protein concentrations were determined by ELISA. The values are shown per million cells (means ± SD of data from four different iHep preparations).

(O) Urea secreted into the media. Cell culture and media harvesting was as in (L–N). The values are shown per million cells (means ± SD of data from four different iHep preparations).

See also Figure S2.

repopulation was also assessed by real-time genomic DNA PCR for *HLA-A54* (Bick et al., 2008) using primers that did not yield any amplicons from the rat genomic DNA template. As an internal control, we used the *36B4* gene (O'Callaghan et al., 2008), which is amplified with equal efficiency from rat and human genomic DNA (see details in the Supplemental Experimental Procedures). By this measurement, human hepatocytes and iHeps constituted 18.2 ± 5.5 and 7.1 ± 4.8 (means ± SD) of the cells in the preconditioned median lobe (Figure 3I) but were below the detectable level in non-irradiated liver lobes. To assess protein secretion by the engrafted human hepatocytes and iHeps, we measured HSA and human transferrin in recipient Gunn rat sera by ELISA. Four to six months after

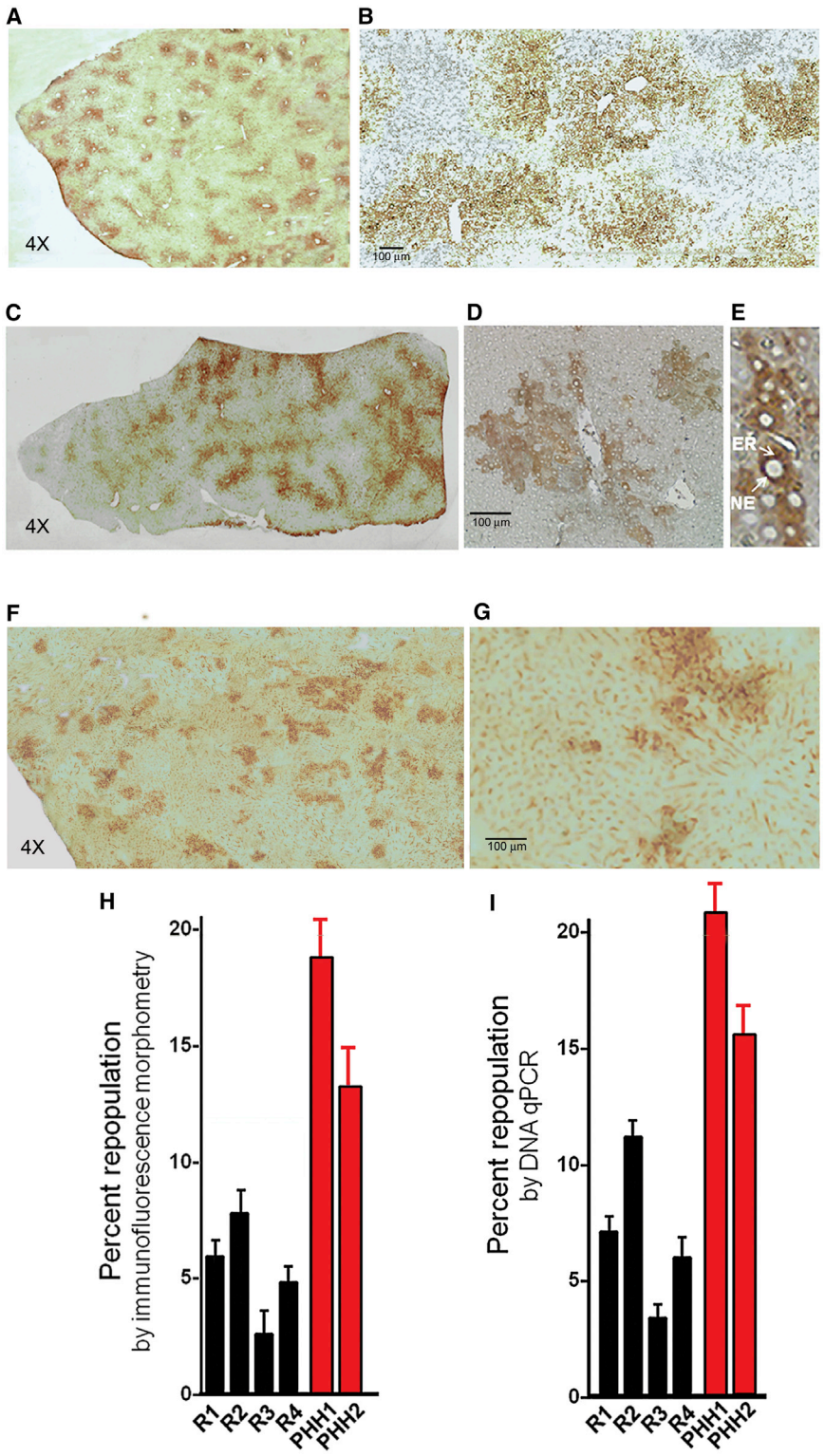

Figure 3. Repopulation of Gunn Rat Livers with Transplanted Human iHep Cells

(A–G) Four to six months after transplantation, livers were harvested from Gunn rats receiving iHeps or primary human hepatocytes (PHH), and cryosections were immunostained with a monoclonal antibody (WP1) that recognizes the carboxy-terminal region of human UGT1A isoforms (A–E) or an HSA-specific antibody (F and G). Representative sections of HIR-preconditioned median lobes are shown.

(A) recipient of PHH. Magnification, 4×.

(B) Section of the same lobe as in (A). Magnification, 10×.

(C) An iHep recipient. Magnification, 4×.

(D) The same lobe. Magnification, 10×.

(E) The same lobe showing characteristic cytoplasmic and nuclear envelope distribution of UGT1A1. Magnification, 40×.

(F) An iHep recipient, stained for HSA. Magnification, 4×.

(G) The same lobe. Magnification, 10×.

(H) Morphometric determination of percent repopulation by human UGT1A1-positive engrafted iHep cells. Each liver lobe was cut into six pieces, and cryosections from each piece were immunostained for human UGT1A1 as in (A). The proportion of hepatocytes that were positively stained was determined by counting ten fields representing 15,000 cells. Data from the median lobes of four individual iHep recipient rats (R1, R2, R3, and R4) and two PHH recipient rats (PHH1 and PHH2) are shown.

(I) Quantification of liver repopulation by iHeps by genomic DNA PCR. Genomic DNA was extracted from homogenates of liver lobes of the four recipient Gunn rats. The repopulating human cells were quantified by qPCR of the *HLA-A54* gene as described in the Supplemental Experimental Procedures. The highly conserved *36B4* gene was amplified as an internal control for both human and rat genes. Data are shown from the median lobes of recipient Gunn rats as in (F).

See also Figure S3.

transplantation, mean HSA and human transferrin levels in the four iHep recipients were 48–73 (60 ± 14) μg/ml and 3.2–8.3 (5.75 ± 2.7) μg/ml, respectively (Figures S3A and S3B). In recipients of primary human hepatocytes, the levels were 232 ± 25 μg/ml and 27 ± 5 μg/ml, respectively (Figures S3A and S3B). These levels were lower than

what might be predicted from the extent of liver repopulation, which may reflect the limitations of xenografting in immunocompetent recipients. Both proteins were undetectable in pre-transplant Gunn rat sera and in sham-treated controls.

To assess the correction of the metabolic abnormality in Gunn rats, we determined hepatic UGT1A1 activity toward bilirubin and serum bilirubin levels in transplant recipients. UGT1A1 activity was undetectable in livers of control Gunn rats. In homogenates of preconditioned median lobes of Gunn rats receiving human hepatocytes, UGT1A1 activities were 3.2 ± 0.4 and 3.6 ± 0.6 nmol/g wet weight/min^{-1} (mean of three determinations ± SD). UGT1A1 activities in iHep recipients were 0.52 ± 0.25 to 2.19 ± 0.38 nmol/g wet weight/min^{-1} (mean ± SD, n = 6), which was 1.5% to 5% of the mean UGT1A1 activity in homogenates of normal human liver (n = 4). In untreated control Gunn rats, serum bilirubin levels increased with age (Figure 4A). In sham-treated controls, serum bilirubin increased to levels above those in untreated Gunn rats for 4–8 weeks, after which the levels equalized. In recipients of human hepatocytes and iHeps, serum bilirubin decreased over time by 70%–80% and 30%–61%, respectively, from pre-transplant levels of 5–7 mg/dl (85–119 μM) (n = 4, $p < 0.01$). The bilirubin levels were lower ($p < 0.01$) than in age-matched controls (n = 6) 6 weeks after transplantation and at all time points thereafter (Figures 4A and 4B).

To confirm the UGT1A1 activity of the engrafted iHeps in vivo, we analyzed the bile from untreated control and transplanted Gunn rats by high-pressure liquid chromatography (HPLC). Untreated Gunn rat bile contained only an unconjugated bilirubin (ucb) peak and no bilirubin glucuronides (Figure 4C). In contrast, bile from the iHep recipients contained bilirubin diglucuronide (bdg) and monoglucuronide (bmg), and the ucb peak was reduced (Figure 4D). bdg and bmg are the predominant species in congeneic normal Wistar-RHA rat bile, which contains only a small amount of ucb (Figure 4E).

Although, in this study, we did not enrich iHeps for ASGPR-expressing cells before transplantation to reduce the risk of transplanting cells with tumor potential, at autopsy, recipient rats did not exhibit teratomas or any other type of tumors despite significant proliferation of the engrafted cells after transplantation, suggesting the absence of residual pluripotent cells after in vitro differentiation of iPSCs.

Therefore, we demonstrated engraftment, proliferation, and function of iHeps following transplantation by immunohistochemical morphometry, qPCR of genomic DNA, UGT1A1 activity in liver homogenates, reduction of serum bilirubin, and excretion of bilirubin glucuronides in the bile. The slightly lower values observed by immunostaining for human UGT1A1 could be because all engrafted iHeps did not express UGT1A1. The function of engrafted iHeps in vivo was also evidenced by the appearance of human proteins in the recipient rat serum. Importantly, because UGT1A1 activity develops postnatally (Odell, 1967), the finding of UGT1A1 activity in the iHeps in vitro and in vivo indicates that, at least in this respect, the iHeps had matured beyond the level of fetal hepatocytes. Although our iHep cells did not exhibit all features of mature hepatocytes, their engraftment and proliferation in the Gunn rat liver provided sufficient UGT1A1 activity to ameliorate jaundice. Human stem cell- or fibroblast-derived hepatocytes have been reported to engraft in murine livers after severe liver injury (Liu et al., 2011). Very recently, iHeps generated by a protocol similar to that used in this study has been shown to engraft in the livers of urinary plasminogen activator transgenic mice and be infectable with hepatitis virus C in vivo (Carpentier et al., 2014). In contrast to these studies, we provide definitive evidence of the engraftment and function of iHeps by reconstitution of a missing hepatocyte-specific enzyme activity and significant amelioration of a metabolic liver defect.

This study required several technical innovations. The ability to limit the delivery of conditioning HIR of the median lobe permitted repopulation of a single liver lobe, leaving the remaining liver unperturbed. Clinical studies using conformal HIR indicate that partial liver irradiation causes much less radiation-induced liver injury than whole-liver irradiation, permitting the safe delivery of higher radiation doses (Dawson and Ten Haken, 2005). Because the engrafted iHeps proliferated significantly only in the preconditioned lobe, 5.1% ± 2.6% repopulation of the median lobe was equivalent to about 1.7% ± 0.99% repopulation of the entire liver. Nonetheless, this level of repopulation was sufficient to significantly reduce the serum bilirubin levels. Although serum bilirubin was not normalized, an equivalent reduction in a clinical setting would be sufficient to protect CN1 patients from developing brain injury and could possibly circumvent the need for prolonged phototherapy.

The ratio between HSA and human transferrin levels in recipient rat sera was lower than that in the culture media of iHeps. This could be because albumin is a negative acute-phase reactant, and its synthesis could be downregulated in the xenotransplanted cells.

Translating this approach to the clinic will require several modifications. The iPSCs will need to be generated under Good Manufacturing Practice conditions, using newer methods of generating iPSCs without transgene integration (Yoshida and Yamanaka, 2011). Because of the small size of the rodent recipients, we delivered regional HIR by surgical exposure of the liver, but, for clinical application,

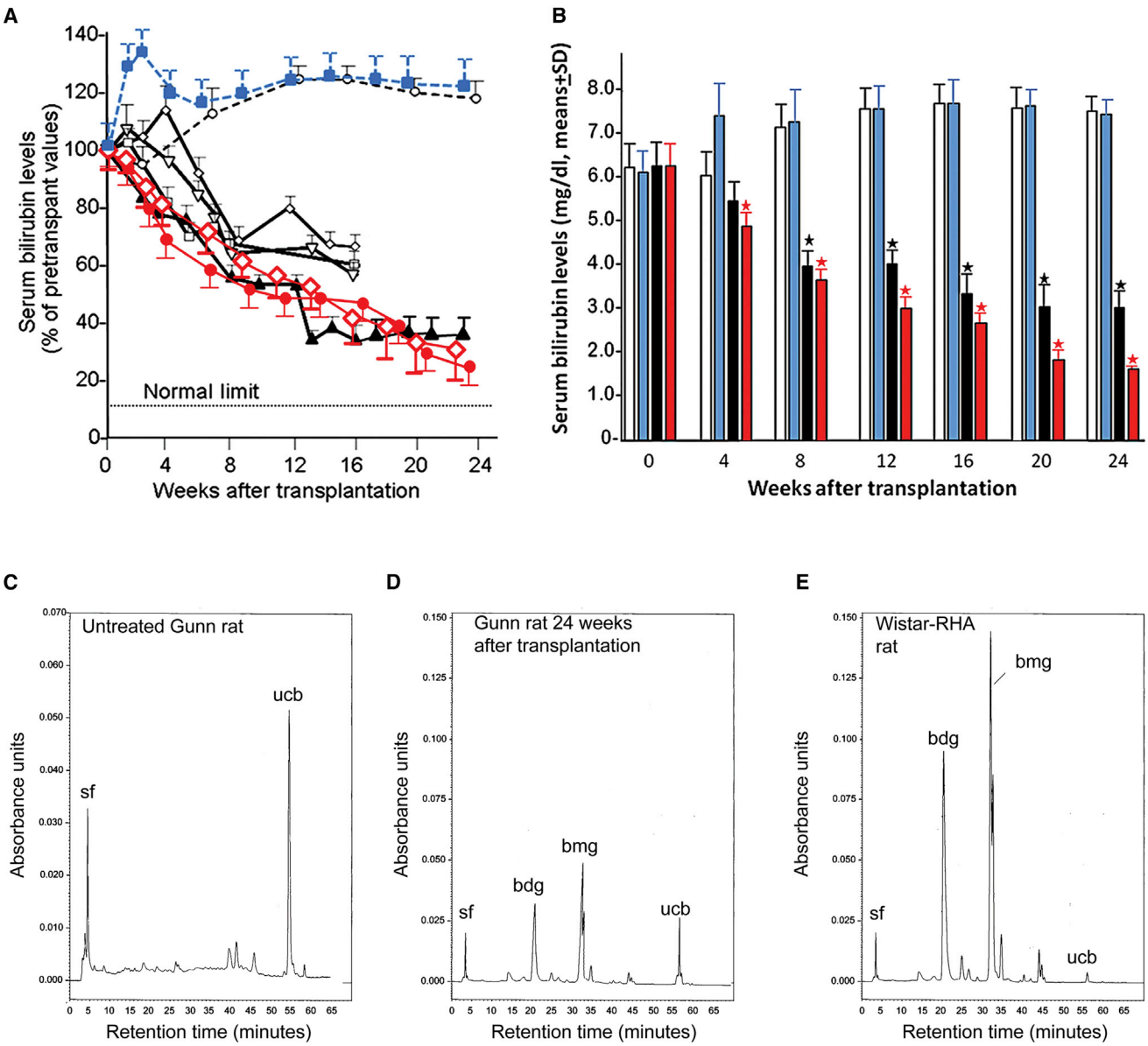

Figure 4. Metabolic Effect of Repopulation

(A) Serum bilirubin levels in the four Gunn rat iHeps (black lines) at the indicated time points after transplantation are shown as percent of pretransplant levels (means ± SD of three determinations for each time point). Dashed black line, untreated age-matched controls (means ± SD of 6 rats); dashed blue line, bilirubin levels in the sham-treated controls; red lines, bilirubin levels after transplantation of primary human hepatocytes; Dotted line, upper limit of serum bilirubin levels in congeneic normal Wistar-RHA rats.

(B) Serum bilirubin levels (mean ± SD) at indicated intervals after transplantation. Open bar, untreated control (n = 6 rats); light blue, sham-operated control (n = 4 rats); black, iHep transplant recipients (n = 4 rats); red, recipients of primary human hepatocytes (n = 2 rats). *$p < 0.02$.

(C–E) High-pressure liquid chromatographic analysis of bilirubin species excreted in the bile of a control Gunn rat, a rat receiving iPSC-derived hepatocytes, and a congeneic normal Wistar RHA rat. sf, solvent front. The absorbance unit scale in (E) is different from that in (F and G).

See also Figure S3.

regional HIR is delivered by conformal irradiation without requiring surgery. Regional irradiation for hepatic repopulation is now in a phase I trial. These readily achievable adaptations should permit the safe application of this transplant strategy for treating CN1 and other inherited liver-based disorders.

EXPERIMENTAL PROCEDURES

iPSC Generation

Normal adult human skin fibroblasts were reprogrammed by retroviral transduction with pluripotency factors, *OCT-4*, *SOX2*, *KLF4*, and *c-MYC*, as described previously (Takahashi and Yamanaka, 2006).

Differentiation of iPSCs to iHep Cells

The iPSCs were differentiated to iHeps as previously described for human ESCs with some modifications (Basma et al., 2009). Briefly, embryoid bodies were not produced, and iPSCs dispersed using dispase were plated in monolayers. Definitive endoderm was generated by exposure to recombinant activin-A (R&D Systems) and fibroblast growth factor 2 (Invitrogen). During the next 8 days, the cells were exposed to HGF (R&D Systems) and DMSO, followed by culturing for 3 days in dexamethasone-containing media (Sigma). At each step, the expression of a series of markers was determined by immunofluorescence staining (see Supplemental Experimental Procedures and Figure 1).

Characterization of iHep Cells

To evaluate the hepatocyte-like characteristics of the iHep cells, we determined the glycogen content and low-density lipoprotein (LDL) and indocyanine green (ICG) uptake by the cells. We also determined the HSA, AFP, and UGT1A1 content; UGT1A1 activity toward bilirubin; as well as secretion of HSA and AAT in the media (see details in the Supplemental Experimental Procedures). For comparison, control primary hepatocytes were isolated from an explanted liver during liver transplantation in a patient with metabolic liver disease.

Statistical Analysis

Serum bilirubin levels in individual rats were determined in triplicate and expressed as percent of pre-transplant values. Data at each time point were compared with those in the control group at the same time point using Student's unpaired two-tailed t test. The number of mice in the control group is represented by n.

SUPPLEMENTAL INFORMATION

Supplemental Information includes Supplemental Experimental Procedures and three figures and can be found with this article online at http://dx.doi.org/10.1016/j.stemcr.2015.04.017.

AUTHOR CONTRIBUTIONS

N.R.C., J.R.C., I.J.F., E.E.B., S.S., and C.G. designed experiments. Y.C., Y.L., X.W., W.Z., V.S., K.T., Z.P., T.T., Y.A., E.T., B.H., C.J.C., and M.G.S. performed cellular, biochemical, and animal experiments. N.R.C., J.R.C., and I.J.F. analyzed the data and wrote the paper.

ACKNOWLEDGMENTS

This work was supported by grants NIH RO1 1RO1 DK092469-01 and a grant from the Oxalosis and Hyperoxaluria Foundation (to N.R.C.); NYSTEM CO24346 and CO26440 (to J.R.C.); NIH RO1 DK48794, AI49472, and DOD W81XWH-09-1-0658 (to I.J.F.); NIH 1PO1 DK 096990-01 (to I.J.F. and J.R.C.); NIH RO1 DK64670 and R21/R33 CA121051 (to C,G,), and NIH P30 DK 41296-26 (to the Liver Pathobiology and Gene Therapy Research Core Center).

Received: April 23, 2013
Revised: April 22, 2015
Accepted: April 29, 2015
Published: June 11, 2015

REFERENCES

Åberg, F., Isoniemi, H., and Höckerstedt, K. (2011). Long-term results of liver transplantation. Scand. J. Surg. *100*, 14–21.

Basma, H., Soto-Gutiérrez, A., Yannam, G.R., Liu, L., Ito, R., Yamamoto, T., Ellis, E., Carson, S.D., Sato, S., Chen, Y., et al. (2009). Differentiation and transplantation of human embryonic stem cell-derived hepatocytes. Gastroenterology *136*, 990–999.

Bick, S.L., Bick, D.P., Wells, B.E., Roesler, M.R., Strawn, E.Y., and Lau, E.C. (2008). Preimplantation HLA haplotyping using tri-, tetra-, and pentanucleotide short tandem repeats for HLA matching. J. Assist. Reprod. Genet. *25*, 323–331.

Bosma, P.J., Chowdhury, N.R., Goldhoorn, B.G., Hofker, M.H., Oude Elferink, R.P.J., Jansen, P.L.M., and Chowdhury, J.R. (1992). Sequence of exons and the flanking regions of human bilirubin-UDP-glucuronosyltransferase gene complex and identification of a genetic mutation in a patient with Crigler-Najjar syndrome, type I. Hepatology *15*, 941–947.

Cai, J., Zhao, Y., Liu, Y., Ye, F., Song, Z., Qin, H., Meng, S., Chen, Y., Zhou, R., Song, X., et al. (2007). Directed differentiation of human embryonic stem cells into functional hepatic cells. Hepatology *45*, 1229–1239.

Carpentier, A., Tesfaye, A., Chu, V., Nimgaonkar, I., Zhang, F., Lee, S.B., Thorgeirsson, S.S., Feinstone, S.M., and Liang, T.J. (2014). Engrafted human stem cell-derived hepatocytes establish an infectious HCV murine model. J. Clin. Invest. *124*, 4953–4964.

Dawson, L.A., and Ten Haken, R.K. (2005). Partial volume tolerance of the liver to radiation. Semin. Radiat. Oncol. *15*, 279–283.

Duan, Y., Ma, X., Zou, W., Wang, C., Bahbahan, I.S., Ahuja, T.P., Tolstikov, V., and Zern, M.A. (2010). Differentiation and characterization of metabolically functioning hepatocytes from human embryonic stem cells. Stem Cells *28*, 674–686.

Fisher, R.A., and Strom, S.C. (2006). Human hepatocyte transplantation: worldwide results. Transplantation *82*, 441–449.

Fox, I.J., Chowdhury, J.R., Kaufman, S.S., Goertzen, T.C., Chowdhury, N.R., Warkentin, P.I., Dorko, K., Sauter, B.V., and Strom, S.C. (1998). Treatment of the Crigler-Najjar syndrome type I with hepatocyte transplantation. N. Engl. J. Med. *338*, 1422–1426.

Guha, C., Parashar, B., Deb, N.J., Garg, M., Gorla, G.R., Singh, A., Roy-Chowdhury, N., Vikram, B., and Roy-Chowdhury, J. (2002). Normal hepatocytes correct serum bilirubin after repopulation of Gunn rat liver subjected to irradiation/partial resection. Hepatology *36*, 354–362.

Lavon, N., Yanuka, O., and Benvenisty, N. (2004). Differentiation and isolation of hepatic-like cells from human embryonic stem cells. Differentiation *72*, 230–238.

Liu, H., Kim, Y., Sharkis, S., Marchionni, L., and Jang, Y.-Y. (2011). In vivo liver regeneration potential of human induced pluripotent stem cells from diverse origins. Sci. Transl. Med. *3*, 82ra39.

Lysy, P.A., Najimi, M., Stéphenne, X., Bourgois, A., Smets, F., and Sokal, E.M. (2008). Liver cell transplantation for Crigler-Najjar syndrome type I: update and perspectives. World J. Gastroenterol. *14*, 3464–3470.

O'Callaghan, N., Dhillon, V., Thomas, P., and Fenech, M. (2008). A quantitative real-time PCR method for absolute telomere length. Biotechniques *44*, 807–809.

Odell, G.B. (1967). "Physiologic" hyperbilirubinemia in the neonatal period. N. Engl. J. Med. *277*, 193–195.

Ozçay, F., Alehan, F., Sevmiş, S., Karakayali, H., Moray, G., Torgay, A., Arslan, G., and Haberal, M. (2009). Living related liver transplantation in Crigler-Najjar syndrome type 1. Transplant. Proc. *41*, 2875–2877.

Roy-Chowdhury, J., Huang, T.J., Kesari, K., Lederstein, M., Arias, I.M., and Roy-Chowdhury, N. (1991). Molecular basis for the lack of bilirubin-specific and 3-methylcholanthrene-inducible UDP-glucuronosyltransferase activities in Gunn rats. The two isoforms are encoded by distinct mRNA species that share an identical single base deletion. J. Biol. Chem. *266*, 18294–18298.

Roy-Chowdhury, N., Kondapalli, R., and Roy-Chowdhury, J. (1993). The Gunn rat: an animal model for inherited deficiency of bilirubin glucuronidation. In Animal Models in Liver Research, C.E. Cornelius, ed. (Academic Press), pp. 149–171.

Roy-Chowdhury, J., Roy-Chowdhury, N., Horslen, S., and Fox, I.J. (2009). Experimental Therapies: Hepatocytes transplantation, gene therapy, and liver assist devices. In Text Book of Gastroenterology, T. Yamada, ed. (Wiley-Blackwell), pp. 2432–2448.

Schwartz, R.E., Linehan, J.L., Painschab, M.S., Hu, W.S., Verfaillie, C.M., and Kaufman, D.S. (2005). Defined conditions for development of functional hepatic cells from human embryonic stem cells. Stem Cells Dev. *14*, 643–655.

Si-Tayeb, K., Noto, F.K., Nagaoka, M., Li, J., Battle, M.A., Duris, C., North, P.E., Dalton, S., and Duncan, S.A. (2010). Highly efficient generation of human hepatocyte-like cells from induced pluripotent stem cells. Hepatology *51*, 297–305.

Song, Z., Cai, J., Liu, Y., Zhao, D., Yong, J., Duo, S., Song, X., Guo, Y., Zhao, Y., Qin, H., et al. (2009). Efficient generation of hepatocyte-like cells from human induced pluripotent stem cells. Cell Res. *19*, 1233–1242.

Takahashi, K., and Yamanaka, S. (2006). Induction of pluripotent stem cells from mouse embryonic and adult fibroblast cultures by defined factors. Cell *126*, 663–676.

Yamanouchi, K., Zhou, H., Roy-Chowdhury, N., Macaluso, F., Liu, L., Yamamoto, T., Yannam, G.R., Enke, C., Solberg, T.D., Adelson, A.B., et al. (2009). Hepatic irradiation augments engraftment of donor cells following hepatocyte transplantation. Hepatology *49*, 258–267.

Yoshida, Y., and Yamanaka, S. (2011). iPS cells: a source of cardiac regeneration. J. Mol. Cell. Cardiol. *50*, 327–332.

Yu, J., Vodyanik, M.A., Smuga-Otto, K., Antosiewicz-Bourget, J., Frane, J.L., Tian, S., Nie, J., Jonsdottir, G.A., Ruotti, V., Stewart, R., et al. (2007). Induced pluripotent stem cell lines derived from human somatic cells. Science *318*, 1917–1920.

Zhou, H., Dong, X., Kabarriti, R., Chen, Y., Avsar, Y., Wang, X., Ding, J., Liu, L., Fox, I.J., Roy-Chowdhury, J., et al. (2012). Single liver lobe repopulation with wildtype hepatocytes using regional hepatic irradiation cures jaundice in Gunn rats. PLoS ONE *7*, e46775.

Stem Cell Reports, Volume *5*

Supplemental Information

Amelioration of Hyperbilirubinemia in Gunn Rats after Transplantation of Human Induced Pluripotent Stem Cell-Derived Hepatocytes

Yong Chen, Yanfeng Li, Xia Wang, Wei Zhang, Vanessa Sauer, Chan-Jung Chang, Bing Han, Tatyana Tchaikovskaya, Yesim Avsar, Edgar Tafaleng, Sanal Madhusudana Girija, Krisztina Tar, Zsuzsanna Polgar, Stephen Strom, Eric E. Bouhassira, Chandan Guha, Ira J. Fox, Jayanta Roy-Chowdhury, and Namita Roy-Chowdhury

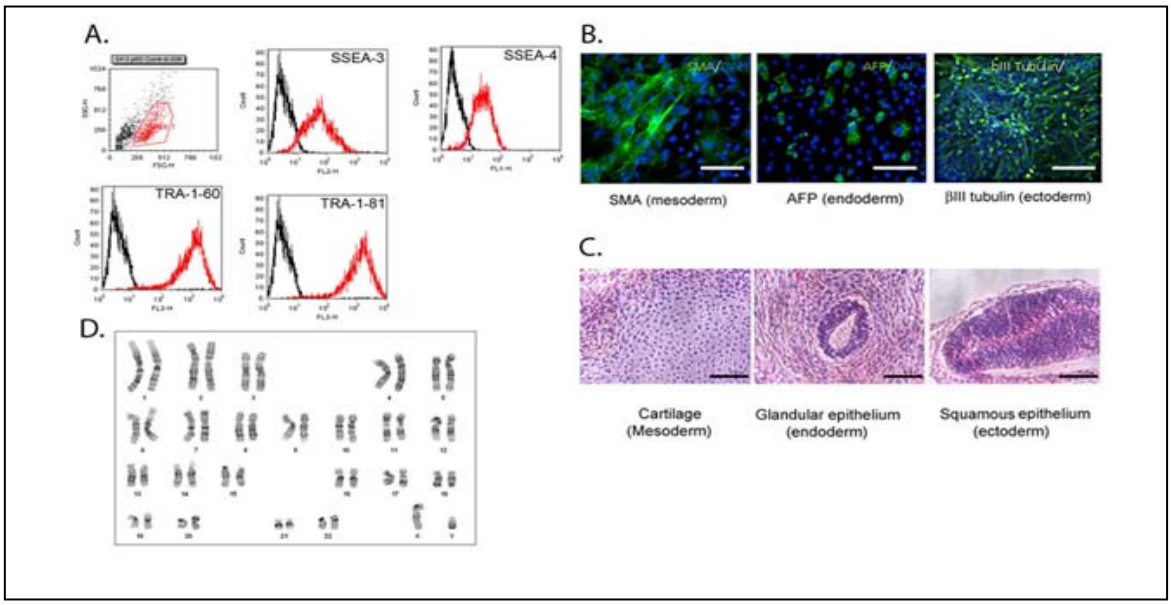

Figure S1. ***Characterization of induced pluripotent stem cells:Related to hiPSCs shown in Figure 1.*** **A.** Flow cytometric analysis of surface markers (SSEA-3, SSEA-4, TRA-1-60, and TRA-1-81) of skin fibroblast-derived iPS cells. Primary mouse monoclonal antibodies specific for the respective surface proteins (red) or control non-immune IgG of the same isotype (black) were used, along with FITC-labeled anti-mouse IgG secondary antibodies. **B.** In vitro differentiation of human iPS cells. Embryoid bodies from iPS cells were plated on gelatin-coated chamber slides, and cultured in ES cell medium for seven days. Staining with anti-smooth muscle (SMA), AFP and anti-β-III tubulin antibodies indicated that the iPS cells could differentiate into cells derived from mesoderm, endoderm and ectoderm, respectively. Magnification 40x. **C.** Teratoma formation: iPS cells were injected intramuscularly in SCID mice. Teratomas were dissected after six weeks. Hematoxylin/eosin staining of teratoma sections show differentiation of iPS cells to tissues derived from mesoderm (cartilage), endoderm (glandular epithelium) and ectoderm (squamous epithelium). Bars = 100 microns. **D.** Karyotyping of iPS cells, performed as described in the Methods section, showed a 44 + X,Y pattern.

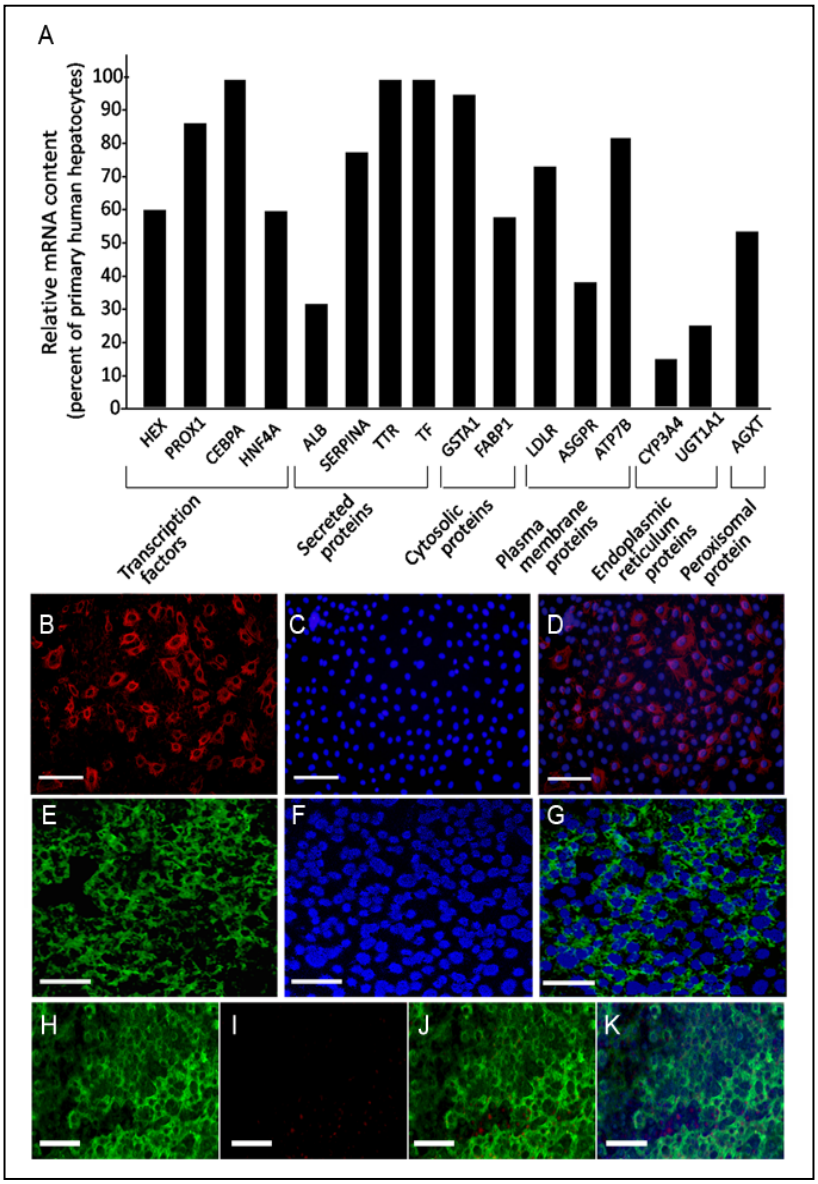

Figure S2. ***mRNA profile of iHep cells, and SOX17, HSA ASGPR expression.*** **Related to Figure 1 and Figure 2.** A. mRNA content of an iHep preparation was compared with that of isolated human hepatocytes that were cryopreserved and thawed before use, using a quantitative RT-PCR array. N-Acetyltransferase 1 (NAT1) mRNA was used as an invariant internal reference. Relative abundances are shown (means of three determinations). The genes are arranged according to their function or intracellular localization of their products. B,

immunofluorescent staining for ASGPR in iHep cells attached to glass slides by cytospin and immunostained without permeabilization, using a human anti-ASGPR1 monoclonal antibody; C, DAPI-stained nuclei of the same field as B; D, overlay of B and C. E, immunofluorescent staining for HSA; F, DAPI-stained nuclei; G, overlay. H-K, Double immunofluorescent staining for HSA and SOX17. H, HSA; I, SOX17; J, HSA/SOX17 overlay; panel J overlaid with DAPI-stained nuclei. Bars=100μm.

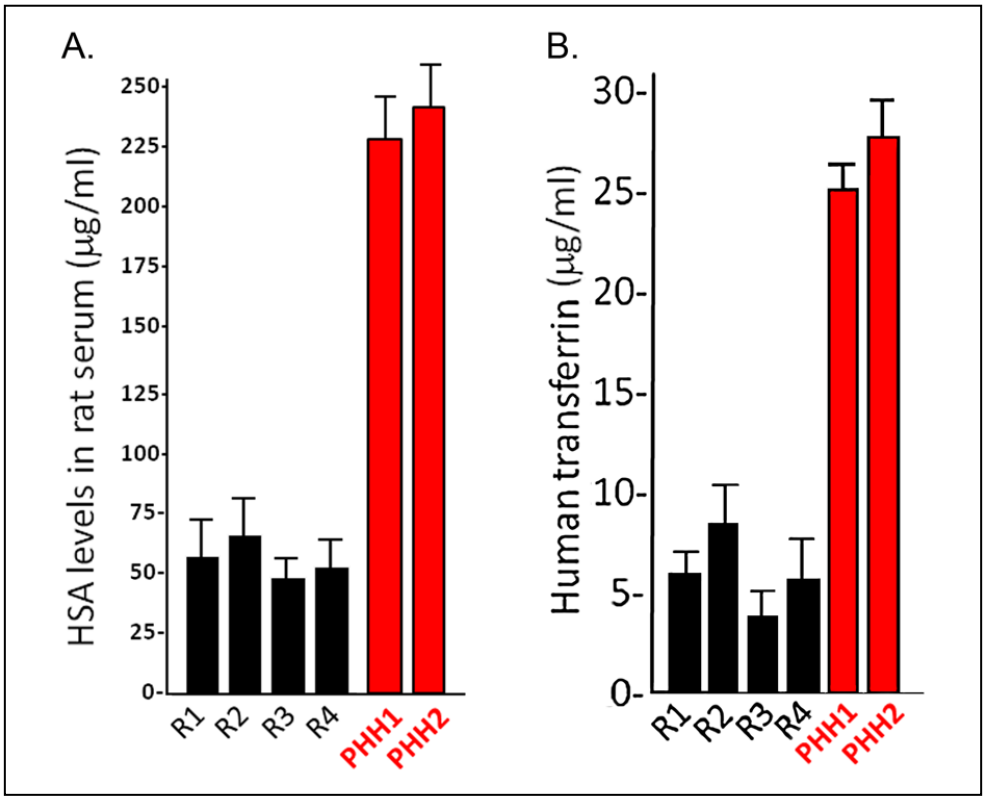

Figure S3. Human serum proteins in the rat plasma. Related to Figure 3 and Figure 4.

Plasma levels of HSA (panel A) and human transferrin (panel B) in four Gunn rats (R1, R2, R3 and R4) that received transplantation of iHep cells (black bars) and two that received primary human hepatocytes (HepCure®, Yecuris) (PHH1 and PHH2: red bars) were determined by ELISA 4 months after transplantation. Each bar represents one recipient Gunn rat, means ± SD of 4 technical replicates of each serum sample are shown.

Supplemental Experimental Procedures

Animals: Inbred Gunn rats were bred and maintained in our colony at Albert Einstein College of Medicine on standard laboratory chow in a climate-conditioned environment and a 12-h light/dark cycle. Both male and female Gunn rats weighing 150-200 g were used. All experiments were performed under humane conditions as approved by the Institutional Animal Care and Use Committee of Albert Einstein College of Medicine.

Generation of iPSCs from human skin fibroblasts: Skin biopsy was obtained from an adult human volunteer after obtaining informed consent in accordance with the Declaration of Helsinki and following the approval of the institutional review board and established in culture. The fibroblasts were reprogrammed to iPSCs by transduction with four retroviruses expressing *OCT-4, SOX2, KLF4,* and *c-MYC* (Takahashi and Yamanaka, 2006) (kindly provided by Dr. S. Yamanaka). The transduced cells were cultured and passaged on Matrigel-coated plates in serum-free hESC culture medium, consisting of DMEM/F12 medium (GIBCO) containing 20% knockout serum replacement supplement (KOSR, GIBCO), 1% insulin-transferrin-selenite (ITS, GIBCO), 2.0 mM L-glutamine (GIBCO), 0.1 mM β-mercaptoethanol (Sigma), 1% non-essential amino acids (GIBCO), 1% penicillin and streptomycin (GIBCO) and 100 ng/ml basic fibroblast growth factor (bFGF, Royan Institute). Three weeks later, hiPSC colonies with hESC-like morphology were released by incubating with 1 mg/ml DMEM/F12 containing collagenase IV (GIBCO), and cultured and passaged on Matrigel-coated plates in the hESC medium (Takahashi and Yamanaka, 2006).

Flow cytometric analysis of hiPSCs and iHep cells: The pluripotency surface markers, SSEA-3, SSEA-4, TRA 1-60, TRA 1-81 that are highly expressed in hESC, and SSEA-1 which is not expressed in hESCs were tested by flow cytometry. iHeps were analyzed for HSA and ASGPR.

Single cell suspension of the hiPSCs or iHeps were prepared by washing the cells twice with CMF-PBS (Ca^{2+}, Mg^{2+}-free PBS) and dissociating with trypLE (10 minutes at 37^{o}C). After washing with CMF-PBS and staining with human-specific antibodies (for HSA, DAKO; for other antigens, BD biosciences) for 30 minutes at 4^{o}C, the cells were washed twice with CMF-PBS + 1% FBS and then analyzed by flow cytometry (FACSCalibur, BD Biosciences, San Jose, CA). Negative controls included isotype-specific IgGs.

Spontaneous differentiation of hiPSCs in vitro: To evaluate whether the iPSCs could give rise to cells of all germ layers in vitro, we generated embryoid bodies (EBs) by plating collagenase-dispersed cells on low-attachment dishes for 48 hours in DMEM/F12 supplemented with 15% knockout serum replacement (KSR) containing 1 mmol/L nonessential amino acids, and L-glutamine. EBs were then transferred to gelatin-coated chamber slides and cultured for seven more days. The cells were fixed with 4% paraformaldehyde, permeabilized with 0.1% Saponin (Sigma) and stained with antibodies against α-fetoprotein, β-III-Tubulin and smooth muscle actin (SMA) (R&D system), using FITC-conjugated secondary antibodies. Human OCT3/4 was stained with a PE-conjugated antibody a (BD Pharmingen). Labeled slides were mounted in Prolong Gold antifade and visualized with a fluorescence microscope (ZEISS, AxioVert 200M).

In vitro differentiation of iPSCs to iHep cells: The iPSCs were differentiated to hepatocyte-like cells as previously described for human ESCs with some modifications (*Basma et al., 2009*). Briefly, the dispersed iPS cells were plated on 5% Growth Factor Reduced Matrigel (R&D Systems, Minneapolis, MN), and cultured for 3 days in DMEM/F12 media containing 100 ng/mL recombinant activin-A (R&D Systems) and 100 ng/mL fibroblast growth factor-2 (Invitrogen). The KSR concentration was 0% for the first 24 hours, 0.2% for the second 24 hours, and 2.0% for the last 24 hours. For the following 8 days, the cells were cultured in

DMEM/F12 containing 10% KSR, 1 mmol/L nonessential amino acids, L-glutamine, 1% dimethyl sulfoxide (Sigma–Aldrich), and 100 ng/mL HGF (R&D Systems Inc), followed by culture for 3 additional days in DMEM/F12 containing 10% KSR, 1 mmol/L nonessential amino acids, L-glutamine, and 10^{-7} mol/L dexamethasone (Sigma–Aldrich).

Karyotype determination: Human iPS cells, grown in Matrigel-coated T25 flasks were processed for Karyotype analysis by Cell Line Genetics (Madison, Wisconsin). Twenty metaphase preparations were counted per karyotype.

Teratoma formation by iPS cells: The hiPSCs were dispersed by collagenase IV treatment, resuspended in ES cell medium, mixed with one-third the volume of matrigel (BD Bioscience) and 10^6 cells were injected into the leg muscles of 6-8 week old SCID mice. After 8 weeks, the visible tumors were dissected, fixed in 10% formalin and paraffin embedded sections were examined after hematoxylin/eosin staining.

Immunofluorescence staining: The cells at different stages of differentiation were fixed with 4% paraformaldehyde in PBS for 20 minutes and then blocked with PBS containing 10% normal donkey serum, 0.1% Triton® X-100 and 1% BSA for 45 minutes at room temperature. After blocking, cells were incubated overnight at 4°C with primary antibodies at dilutions indicated: hOCT3/4 (R&D system) and FOXA2 (R&D system) 10μg/ml, AFP (Dako) and serum albumin (hALB, Dako) 1:100, cytokeratin 18 (hCK18, Santa Cruz) and asialoglycoprotein receptor (hASGPR Santa Cruz) 1:200. After this the cells were incubated with secondary antibodies conjugated with FITC or Rhodamine at room temperature in the dark for one hour. Between each step, cells were washed with PBS containing 0.1% BSA.

Western blot for human AFP, albumin and UGT1A1: Cell homogenates (25 μg protein) were subjected to Western blot analysis using specific antibodies against human ALB (Dako), AFP

(Dako) and a monoclonal antibody (WP1) that recognizes human UGT1A group of enzymes (Peters et al., 1987). The immunoreactive bands were visualized using an enhanced chemiluminescence system (Pierce).

Cytochemical staining for glycogen: After the final differentiation step, the cells were stained with the periodic acid Schiff (PAS) reagent.

Indocyanine green and low-density lipoprotein (LDL) uptake: Uptake of the organic anion indocyanin green (ICG, Sigma) was studied as described (Yamada et al., 2002). LDL uptake was determined using DiI-LDL as described (Roy-Chowdhury et al., 1991).

UGT1A1 activity of primary human hepatocytes and iHep cells toward bilirubin: After dexamethasone treatment, the cells were scraped and homogenized. UGT1A1 was activated by incubation with 5mg/ml digitonin suspension, and bilirubin glucuronidating activity was measured as described (Roy-Chowdhury et al., 1982). For this purpose, fresh frozen primary human hepatocytes were purchased from Triangle Research Labs, Research Triangle Park, NC.

Secretion of human proteins and urea in the media: iHeps and primary hepatocytes isolated from an explanted liver were plated in Matrigel-coated 6-well plates at 80% confluency and cultured in serum-free media for 16 hours. Human proteins secreted in the media were determined by ELISA using antibodies against human ALB and human α1-antitrypsin (Ding et al., 2011) (AAT, Bethyl Laboratories, Montgomery, TX). Urea secreted in the media was assayed colorimetrically using a kit (Thermo, MA).

Transplantation of iHep cells or human hepatocytes into Gunn rats: As Gunn rats are immune competent, we developed a special immunosuppression regimen to prevent xenograft rejection. Recipient Gunn rats were injected with tacrolimus 2 mg/kg, subcutaneously daily, beginning 7 days before transplantation (Basma et al., 2009). To provide a proliferative advantage to the

transplanted cells, we used hepatic irradiation (HIR) (50 Gy), which reduces the mitotic capacity of the host hepatocytes without causing large scale cell death. For mitotic stimulation, an adenovector expressing human HGF (Ad-HGF) was injected ($1x10^{12}$ particles, intravenously) as described (Roy-Chowdhury et al., 1982, Jian et al., 2008). The mitotically competent transplanted hepatocytes proliferate in response to HGF, progressively replacing the host hepatocytes (Jian et al., 2008). Taking advantage of the region-specificity of X-irradiation, we limited HIR (50Gy) to the median liver lobe (~33% of the liver mass), leaving the remaining liver unaffected, as would be performed for safety in the clinical setting. We have observed previously that repopulation of a single Gunn rat liver lobe with wildtype rat hepatocytes is sufficient to normalize serum bilirubin levels (Zhou et al., 2012). One day after HIR, we transplanted iHep cells by intrasplenic injection (Guha et al., 2002). Based on a prior determination of cell viability and the percentage of cells positive for HSA, we transplanted $2x10^6$ HSA positive viable iHep cells. For comparison, we transplanted $2x10^6$ viable cryopreserved human hepatocytes isolated by collagenase perfusion of the livers of fumarylacetoacetate hydrolase (Fah) knockout, and the Rag2 and Il2rγ deficient mice (FRG) repopulated with human hepatocytes (HepCure, Yecuris, Tualtin, OR). Two control groups were studied also: (1) six age-matched Gunn rats receiving tacrolimus and Ad-HGF, but no other treatment; (2) four sham operated controls that received HIR to the median lobe, but no transplantation.

Immunocytochemistry and immunofluorescence staining of transplanted iHeps: After 4-6 months of transplantation liver tissues were fixed, cut and stained immunohistochemically using the monoclonal antibody WP1 against human UGT1A isoforms (Peters et al., 1987). Livers of untreated Gunn rats were used as control.

Quantification of liver repopulation by iPSC-Heps by genomic DNA PCR: To determine the proportion of iHeps or primary human hepatocytes in the recipient liver, a standard curve was prepared by mixing human liver homogenates into Gunn rat liver homogenates (10 ml/gm liver wet weight) at various ratios from 0% (i.e. only Gunn rat liver homogenate) to 100% (i.e. only human liver homogenate). Genomic DNA was extracted from homogenates of the preconditioned and other liver lobes. The human *HLA-A54* gene was quantified by DNA PCR using the following amplimers: Forward: 5'-GCTCAGTTCCAGTTGCTTG-3'; Reverse: 5'-GCAGTGAGCCAAGATTGCAC-3'. The PCR mixture contained Express SYBR GreenER Super Mix with Premixed ROX) 12.5 μl, genomic DNA template 100 ng in 1 μl, forward and reverse primer 10 μmoles and double distilled water 10 μl. PCR was performed up to 40 cycles using the following program: 50°C 2 min and 95°C 10 min, followed by 95°C 15 sec and 60°C. As an internal standard, we amplified the *36B4* gene using amplimers that yield amplicons from human and rat genomic DNA with equal efficiency. The primers were as follows: Forward: 5'-GCGACCTGGAAGTCCAACTAC-3'; reverse: 5'-ATCTGCTGCATCTGCTTGG-3'. The extent of liver repopulation was calculated by fitting the results of qPCR on the DNA extracted from liver lobes of the recipient rat to the standard curve generated from the mixtures of Gunn rat and human liver homogenates.

Measurement of serum bilirubin: Serum samples at various time points before and after transplantation were measured (Jendrassik and Grof, 1938). Serum bilirubin levels of age-matched control Gunn rats were determined for comparison.

Assay of human proteins in recipient rat sera: Human serum albumin and alpha-1 antitrypsin concentrations were determined in the sera of recipient Gunn rats by ELISA, employing human-specific antibodies as described (Bumgardner et al., 1998)).

UGT1A1 activity in the liver of the transplant recipient Gunn rats: UGT1A1 activity toward bilirubin was assayed in the liver homogenates of the transplant recipient Gunn rats and the untreated controls as described (Roy-Chowdhury et.al.,1981).

Analysis of pigments excreted in bile: Bile samples were collected by cannulating the bile ducts with PE10 catheters and the bilirubin species excreted in bile were analyzed by High Pressure Liquid Chromatography as described (Roy-Chowdhury et al., 1982). Bile samples from untreated Gunn rats and congeneic wildtype Wistar-RHA rats were used as controls.

Supplemental References

Bumgardner, GL., Heininger, M., Li, J., Dongyuan, X ., Parker-Thornburg, J., Ferguson, RM.and Orosz, CG. (1998) A functional model of hepatocytes transplantation for in vivo immunologic studies.Transplantation, **65**, 53-61.

Ding, J., Yannam, GR., Roy-Chowdhury, N., Hidvegi, TH., Basma, H., Rennard, SI., Wong, RJ., Avsar, Y., Guha, C., Perlmutter, DH., Fox, IJ., and Roy-Chowdhury, J. (2011) Spontaneous hepatic repopulation in transgenic mice expressing mutant human alpha 1-anti-trypsin by wild-type donor hepatocytes. J. Clin. Invest. **121**,1930-1934.

Jendrassik, L., and Gróf, P. (1938) Vereinfachte photometrische methoden zur bestimmung des blut-bilirubins. *Biochem. Zeitschrift.* **297**: 82-89.

Jian, J., Salido, EC., Guha, C., Wang X, Moitra, R., Liu, L., J. Roy-Chowdhury, J., and Roy-Chowdhury, N. (2008) Correction of Hyperoxaluria by liver repopulation with hepatocytes in a mouse model of primary hyperoxaluria type -1. Transplantation, **85,** 1253-1260.

Peters, W., Allebes, WA.,Jansen, PLM., Poels, LG., Capel, PJA. (1987) Characterization and tissue specificity of a monoclonal antibody against human uridine 5'-diphosphate glucuronosyltransferase. Gastroenterology **93**, 162-169.

Roy-Chowdhury, J., Grossman, M., , S., Roy-Chowdhury, N., Baker, JR., Wilson, JM. (1991) Long term improvement of hypercholesterolemia after *ex vivo* gene therapy in LDL-receptor deficient rabbits. Science **254**, 1802-1805.

Roy-Chowdhury, J., Roy-Chowdhury, N., Gartner, U., Wolkoff, AW., and Arias, IM. (1982) Bilirubin diglucuronide formation in intact rats and in isolated Gunn rat livers. J. Clin. Invest. **699**: 595-603.